Deep-Sea Research II 58 (2011) 2647–2660

Contents lists available at ScienceDirect

Deep-Sea Research II

journal homepage: www.elsevier.com/locate/dsr2

Dissolved aluminium in the Southern Ocean

R. Middag [a,*], C. van Slooten [a], H.J.W. de Baar [a,b], P. Laan [a]

[a] Royal Netherlands Institute for Sea Research (Royal NIOZ), P.O. BOX 59, 1790 AB Den Burg, Texel, The Netherlands
[b] Department of Ocean Ecosystems, University of Groningen, Groningen, The Netherlands

ARTICLE INFO

Article history:
Received 8 March 2011
Accepted 8 March 2011
Available online 12 March 2011

Keywords:
Trace metals
GEOTRACES
Southern ocean
Dissolved aluminium
Aluminium cycle

ABSTRACT

Dissolved aluminium (Al) occurs in a wide range of concentrations in the world oceans. The concentrations of Al in the Southern Ocean are among the lowest ever observed. An all-titanium CTD sampling system makes it possible to study complete deep ocean sections of Al and other trace elements with the same high vertical resolution of 24 depths as normal for traditional CTD/Rosette sampling. Overall, 470 new data points of Al are reported for 22 full depth stations and 24 surface sampling positions along one transect. This transect consisted of 18 stations on the zero meridian proper from 51°57′ S until 69°24′S, and 4 stations somewhat to the northeast towards Cape Town from 42°20′S, 09°E to 50°17′S, 01°27′E. The actual concentrations of Al in the Southern Ocean were lower than previously reported. The concentration of Al in the upper 25 m was relatively elevated with an average concentration of 0.71 nM (n=22; S.D.=0.43 nM), most likely due to atmospheric input by a suggested combination of direct atmospheric (wet and dry) input and indirect atmospheric input via melting sea ice. Below the surface waters there was a distinct Al minimum with an average concentration of 0.33 nM (n=22; S.D.=0.13 nM) at an average depth of 120 m. In the deep southernmost Weddell Basin the concentration of Al increased with depth to ~0.8 nM at 4000 m, and a higher concentration of ~1.5 nM in the ~4500–5200 m deep Weddell Sea Bottom Water. Over the Bouvet triple junction region, where three deep ocean ridges meet, the concentration of Al increased to ~1.4 nM at about 2000 m depth over the ridge crest. In the deep basin north of the Bouvet region the concentration of Al increased to higher deep values of 4–6 nM due to influence of North Atlantic Deep Water. In general the intermediate and deep distribution of Al results from the mixing of water masses with different origins, the formation of deep water and additional input from sedimentary sources at sea floor elevations. No significant correlation between Al and silicate (Si) was observed. This is in contrast to some other ocean regions. In the Southern Ocean the supply of Al is extremely low and any signal from Al uptake and dissolution with biogenic silica is undetectable against the high dissolved Si and low dissolved Al concentrations. Here the Al–Si relation in the deep ocean is uncoupled. This is due to the scavenging and subsequent loss of the water column of Al, whereas the concentration of Si increases in the deep ocean due to its input from deep dissolution of biogenic diatom frustules settling from the surface layer.

1. Introduction

Dissolved aluminium (hereafter Al) occurs in a wide range of concentrations in the world oceans, from as low as 0.1 nM in surface waters of the Pacific Ocean (Orians and Bruland, 1986; Measures et al., 2005) to 174 nM in the Mediterranean Sea (Hydes et al., 1988). Aluminium has been shown to have a quite complex biogeochemistry. Moreover, its residence time is much shorter in the surface ocean than in the deep ocean (Orians and Bruland, 1985, 1986). Fluvial inputs of Al to the open ocean are negligible due to estuarine removal processes (Mackin and Aller, 1984; Tria et al., 2007 and references therein). Maring and Duce (1987) suggested aeolian dust to be the main source of Al to the open ocean, which has since then been confirmed convincingly (Tria et al., 2007 and references therein). In the North West Atlantic Ocean, and also on a global scale, concentrations of Al in the surface ocean have been related to atmospheric dust input (e.g. Gehlen et al., 2003; Kramer et al., 2004; Han et al., 2008). In the surface ocean, Al has a short residence time of only 4 weeks to 4 years (Orians and Bruland, 1986) due to removal from the water column. Several studies have suggested passive, inorganic sorption onto particle surfaces as an important removal mechanism (e.g. Hydes, 1979; Moore and Millward, 1984; Orians and Bruland 1985, 1986). However, there are also indications of active

* Corresponding author. Tel.: +31 222 369 464.
E-mail address: rob.middag@nioz.nl (R. Middag).

0967-0645/$ - see front matter © 2011 Elsevier Ltd. All rights reserved.
doi:10.1016/j.dsr2.2011.03.001

uptake of Al by diatoms. These are the nutrient-like increase with depth of Al at several locations (Stoffyn, 1979; Hydes et al., 1988; Chou and Wollast, 1997), as well as the significant correlations often found between dissolved Al and silicate (Mackenzie et al., 1978; Hydes et al., 1988; Kramer et al., 2004; Middag et al., 2009). Moreover, Gehlen et al. (2002) have shown that Al is structurally associated with the biogenic silica of diatom frustules, consistent with earlier studies of Al incorporation in opal frustules of diatoms (Van Bennekom et al., 1989, 1991; Van Beusekom and Weber, 1992). In the deep ocean the concentrations of Al have been suggested to be quasi-conservative (Measures and Edmond, 1990) due to less scavenging. Deep ocean residence times have been estimated to be between 50 and 200 years (Orians and Bruland, 1985, 1986). Additional input in the deeper water column has been suggested via diffusion from the sediments (Hydes, 1977), pressure dependent solubility of Al-containing particles (Moore and Millward, 1984) and shelf water input via deep slope convection (Measures and Edmond, 1992; Middag et al., 2009).

An all-titanium CTD sampling system (De Baar et al., 2008) allows to study complete deep ocean sections of trace elements with the same high spatial resolution of 24 depths as for traditional CTD/Rosette sampling. Here are presented the distributions of Al along a section at (or nearby) the zero meridian (0°W) determined in February–March 2008, during expedition ANT XXIV/3 aboard R.V. Polarstern. This expedition was part of the International Polar Year—Geotraces programme (www.geotraces.org) with the objective to: 'identify processes and quantify fluxes that control the distributions of key trace elements and isotopes in the ocean, and to establish the sensitivity of these distributions to changing environmental conditions' (Geotraces Science Plan, 2006). Among others, also the distributions of iron (Fe) (Klunder et al., 2011), manganese (Mn) (Middag et al., 2011), zinc (Croot et al., 2011), cadmium and its isotopes (Abouchami et al., in press) and the speciation of zinc (Baars and Croot, 2011) and Fe (Thuróczy et al., 2011) were successfully measured during this expedition. The distributions of Al are compared with the distributions of other variables, notably the salinity and the potential temperature, to gain insight in the sources and cycling of Al in the Southern Ocean and in relation to the world oceans.

2. Methods

2.1. Sampling and filtration

The low density polyethylene bottles (LDPE, Nalgene) used for the storage of reagents and samples were cleaned according to an intensive three-step cleaning procedure as described in Middag et al. (2009). After cleaning, LDPE bottles are suitable for use in the analysis of Al (Brown and Bruland, 2008). Seawater was collected using 24 internally Teflon-coated PVC 12 l GO-FLO samplers (General Oceanics Inc.) mounted on an all-titanium frame that was connected to a Kevlar wire and controlled from onboard (De Baar et al., 2008). Samples were taken at 22 stations along the transect. There were 18 stations on the zero meridian proper from 51°57′ S until 69°24′S near the edge of the continental ice-sheet, and 4 stations on the extension towards Cape Town somewhat to the east in the South East Atlantic Ocean from 42°20′S, 09°E to 50°17′S, 01°27′E (Fig. 1). The 22 deployments of the all-titanium CTD sampling system with 24 GO-FLO samplers resulted in a total of 487 samples that were analysed for Al. This is somewhat less than the theoretical maximum of 528 due to the water requirements of other cruise participants and the occasional malfunctioning of a GO-FLO sampler. Of the 487 samples analysed for Al, 41 samples (8.4%) were suspected outliers and therefore not further used in the data analyses and figures presented. Suspected outliers were labelled as such based on three criteria. When for the sampled GO-FLO the nutrient data (see text Section 2.4.) were anomalous for that depth, indicating closing at the wrong depth, the sample was marked as suspected outlier. In case the trace metal data (Al, Mn and Fe) were elevated for the same GO-FLO for more than one cast, indicating a contaminated GO-FLO sampler, the sample was also marked as a suspected outlier. The third criterion was when 1 data point of Al gave anomalous result for its depth considering the data points at shallower and greater depths. These anomalous data points were identified by visually inspecting the vertical profiles for data points that would not fit in the profile shape. Subsequently, this data point was compared with the values of potential temperature, salinity, nutrients, Mn and Fe to see if those showed a similar trend. If this was the case the data point was left in, if not the following test was applied; a linear regression was determined between the concentrations of Al below and above the suspect data point (2 above and 2 below if possible) versus depth. With the linear regression equation the 'theoretical' concentration was calculated for the depth with the anomalous concentration of Al. When this calculated value was more than 25% lower than the measured value, it was marked as a suspected outlier and not further used in the calculations or graphs.

The complete relational database includes specific flags for suspected outlier values and will be available at the international GEOTRACES data centre (http://www.bodc.ac.uk/geotraces/) and is also available as an Electronic annex with this paper. In between the 22 stations for trace metals and nutrients, another 30 stations were sampled with the regular CTD/Rosette also for nutrients and for other variables (see electronic Supplement).

Samples for Al analysis were taken from the GO-FLO samplers in a class 100 clean room environment. The water was filtered directly from the GO-FLO sampler over a 0.2 μm filter capsule (Sartrobran-300, Sartorius) under nitrogen pressure (1.5 atm). Therefore all data reported in this paper is dissolved Al. The filtered seawater samples were collected in cleaned LDPE sample bottles (125 ml) from each GO-FLO bottle. All sample bottles were rinsed five times with the sample seawater.

Underway surface sampling (target depth of 1.5 m) was conducted during transit between stations from south of 66°01′S onwards until 69°35′S near the continental ice edge. This was done with a towed epoxy-coated stainless steel torpedo deployed off a crane arm on the starboard side of the ship. Water was pumped aboard with an Almatec A-15 Teflon diaphragm pump. A total of 24 samples were sampled inside the same class 100 clean room environment (see above) by in-line filtration over a filter capsule containing a 0.4 μm pre-filter and a 0.2 μm end-filter (Sartrobran P 0.2 μm, Sartorius).

Unfiltered samples for nutrients were collected in high density polyethylene bottles that were rinsed three times with sample water. Samples were stored in the dark at 4 °C prior to analysis (see text Section 2.4.).

2.2. Analyses of dissolved Al

The analyses of dissolved Al were performed on shipboard after the method developed by Resing and Measures (1994) with improvements by Brown and Bruland (2008). This method is a flow injection analysis, based on the fluorescence from the reaction between lumogallion and Al. Samples were stored in a refrigerator (4 °C) and analysed usually within 24 h after sampling but always within 36 h. Samples were acidified 1 h before the start of a run of 10 samples with 12 M ultraclean HCl (Baseline® Hydrochloric Acid, Seastar Chemicals Inc.) to a pH of 1.8. In the flow injection system the samples were buffered inline

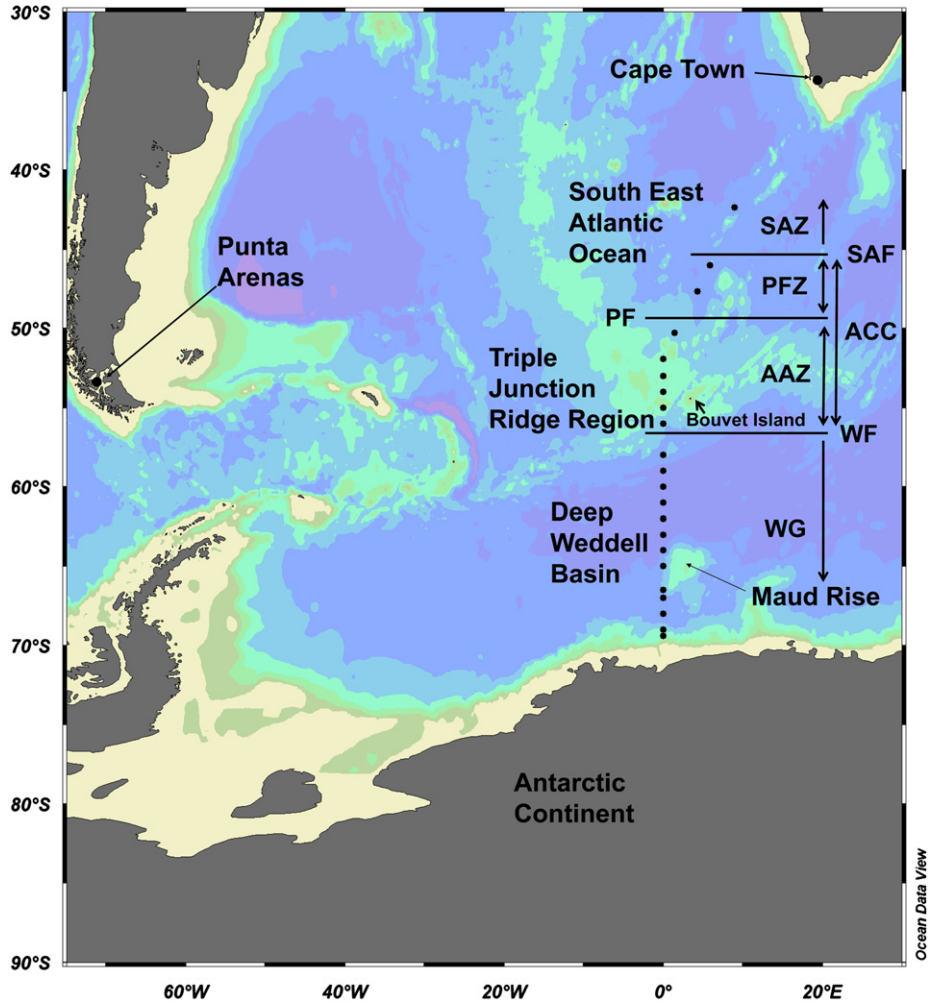

Fig. 1. Trace metal sampling stations along the zero meridian and in the South East Atlantic Ocean during cruise ANT XXIV/3 from 10 February until 16 April 2008 from Cape Town (South Africa) to Punta Arenas (Chile) aboard R.V. Polarstern. Abbreviations in alphabetical order: ACC: Antarctic Circumpolar Current; PF: Polar Front; PFZ: Polar Frontal Zone; SAF: Sub Antarctic Front; SAZ: Sub Antarctic Zone; WF: Weddell Front; and WG: Weddell Gyre.

to a pH of 5.5 ± 0.1 with ultraclean 2 M ammonium acetate buffer. This buffer was produced by diluting a saturated solution of ammonium acetate crystals to a 2 M solution with MQ (Millipore Milli-Q deionised water $R > 18.2\ \mathrm{M\Omega\ cm^{-1}}$). The pH was subsequently adjusted to be between 8.8 and 8.9 with ultraclean ammonium hydroxide.

The buffered sample was pre-concentrated for 200 s on a Toyopearl AF-Chelate 650 M (TosoHaas, Germany) column. Next the column was rinsed for 60 s with MQ water to remove interfering salts. The Al was subsequently eluted from the column with 0.10 M HCl (Suprapure, Merck) during 250 s. The eluate of Al in HCl entered the reaction stream that consisted of a lumogallion (Pfaltz & Bauer) solution in 4 M ammonium acetate buffer. The 4 M buffer was produced similar to the 2 M buffer (see above), but with the pH adjusted to be between 6.4 and 6.5 and the lumogallion was a 4.8 mM solution in MQ. The mixing of the HCl and the buffer results in a reaction pH between 5.3 and 5.4 at which an Al–lumogallion chelate complex is formed, which can be detected by its fluorescence. The complex was mixed in a 10 m reaction coil placed in a water bath of 50 °C. Hereafter a 5% Brij-35 (Merck) solution in MQ was added to increase the sensitivity (Resing and Measures, 1994) and mixed in a 3 m length mixing coil. Afterwards the emission of the fluorescent complex was detected on a FIA-lab PMT-FL detector with a 510–580 nm emission filter and a 480–490 nm excitation filter. Concentrations of Al were calculated in nanomol L^{-1} (nM) from the peak heights.

2.3. Calibration of Al

The system was calibrated using standard additions from a 5000 nM Al stock solution (Fluka) to filtered acidified seawater of low (< 0.5 nM) Al concentration that was collected in the Antarctic Ocean. A six-point calibration line (0, 1, 2, 4, 6 and 8 nM Al standard additions) and blank determination were made every day. The 3 lowest points (0, 1 and 2 nM Al standard additions) of the calibration line were measured in triplicate and the 3 highest points (4, 6 and 8 nM Al standard additions) in duplicate in order to add more weight to the lower part of the calibration line. The blank was determined by plotting the signals of increasing pre-concentration times (30, 60, 120, 180 and 240 s) of the filtered acidified seawater of low (< 0.5 nM) Al concentration also used for the calibration. A line was fitted through these data points and the intercept of the line taken as the blank, which was 0.18 nM (S.D. = 0.02 nM; $n = 23$). The value of 0.2 nM was the maximum allowed blank before starting a series of analyses. The limit of detection, defined as three times the standard deviation of the lowest concentration observed, was 0.07 nM. The flow injection system was cleaned every day by rinsing with a 0.5 M HCl solution.

A check sample was measured in triplicate every day. This check sample was a sub-sample of a 25 L volume of filtered seawater that was taken at the beginning of the cruise in the South East Atlantic Ocean. This check sample was filtered and acidified as the samples. The relative standard deviation (i.e. the precision) of this replicate analysis seawater sample that was analysed 36 times on different days in triplicate was 3.16%. The relative standard deviation on single days was on average 1.5%. The average concentration of Al of this check sample was 3.56 nM and the deviation from this average for a given measuring day was used as a correction factor. This correction factor is on average implicitly 1 and the standard deviation was 0.03. To verify whether this correction was decreasing the inter-daily variability in the dataset, every day a sample, which was collected and measured the previous measuring day, was analysed once again. The deviation between the concentrations measured on the different days decreased from 4.8% to 3.5%, indicating the data correction is beneficial. Moreover, samples of the SAFe intercalibration programme (Johnson et al., 2007) were analysed in triplicate (Table 1). Results for both SAFe Surface (S) of 1.68 ± 0.04 nM ($n=8$) and SAFe deep (D2) of 1.01 ± 0.08 nM ($n=17$) from 1000 m water are in good agreement with the values found by Brown and Bruland (2008) of 1.67 ± 0.02 nM and 0.99 ± 0.02 nM, respectively.

2.4. Additional analyses

The salinity (conductivity), temperature and depth (pressure) were measured with two different CTD's of the same type (Seabird SBE 911+), one from the Netherlands Institute for Sea Research (NIOZ) and other from the Alfred Wegener Institute (AWI). Both had been calibrated before and after the expedition by the company (Seabird) and mutual agreement was excellent. Moreover, the conductivity sensors were calibrated during the cruise against salinity samples measured onboard. The inorganic major nutrients nitrate, nitrite, phosphate and silicate ($Si(OH)_4$), from here on Si, were determined following procedures after Grasshoff et al. (1983).

Table 1
Results of analysis of Al (nM) for SAFe samples during the cruise ANT XXIV/3 from 06 February until 16 April 2008 aboard Polarstern. Results for both SAFe Surface (S) (average of 1.68 ± 0.04 nM ($n=8$)) and SAFe deep (D2) (average of 1.01 ± 0.08 nM ($n=17$)) from 1000 m water are in good agreement with the values found by Brown and Bruland (2008) of 1.67 ± 0.02 and 0.99 ± 0.02 nM, respectively.

Date	SAFe Sample	Al (nM)	Standard deviation (nM)
21/02/2008	SAFe S 426	1.59	*0.030*
23/02/2008	SAFe S 426	1.69	*0.005*
24/02/2008	SAFe S 426	1.66	*0.025*
26/02/2008	SAFe D2 524	1.04	*0.029*
27/02/2008	SAFe D2 524	1.02	*0.025*
06/03/2008	SAFe D2 121	0.93	*0.005*
07/03/2008	SAFe D2 121	0.99	*0.007*
10/03/2008	SAFe S 247	1.70	*0.063*
11/03/2008	SAFe S 247	1.73	*0.054*
12/03/2008	SAFe S 247	1.71	*0.033*
13/03/2008	SAFe S 247	1.67	*0.049*
16/03/2008	SAFe D2 19	0.96	*0.024*
18/03/2008	SAFe D2 19	1.01	*0.032*
19/03/2008	SAFe D2 19	1.02	*0.015*
22/03/2008	SAFe S 113	1.68	*0.021*
24/03/2008	SAFe D2 7	1.07	*0.029*
26/03/2008	SAFe D2 7	1.04	*0.092*
28/03/2008	SAFe D2 7	1.13	*0.033*
29/03/2008	SAFe D2 8	0.88	*0.013*
02/04/2008	SAFe D2 416	0.99	*0.067*
03/04/2008	SAFe D2 416	1.16	*0.005*
05/04/2008	SAFe D2 416	1.03	*0.026*
07/04/2008	SAFe D2 347	0.87	*0.019*
08/04/2008	SAFe D2 347	1.06	*0.050*
09/04/2008	SAFe D2 347	1.07	*0.025*

3. Results

3.1. Hydrography

Several fronts exist, in southward direction the Subtropical Front (STF), the Sub-Antarctic Front (SAF), the Polar Front (PF), the Southern Boundary of the Antarctic Circumpolar Current Front (SB ACC or SBdy) and the Weddell Front (WF). South of the SAF the Antarctic Circumpolar Current (ACC) flows eastward, extending unbroken around the globe. Within the ACC the mentioned PF is found (Fig. 2). A more detailed description of the hydrography can be found in the electronic supplement.

The Subtropical Front was located to the north of the sampled transect. The zone between the Subtropical Front and the SAF is known as the Sub-Antarctic Zone (SAZ). The SAF was located between the stations at 44°40′S, 07°06′W and 46°S, 5°53′W (Fig. 2). About 3° further south, between the stations at 48°55′S, 2°48′E and 50°16′S, 1°27′E, the PF was observed (Fig. 2). The zone between the SAF and the PF is known as the Polar Frontal Zone (PFZ). The southern boundary of the ACC (SB ACC, also referred to as SBdy (e.g. Barré et al., 2008)) was located between the stations at 55°30′S, 00°E and 56°S, 00°E (Fig. 2). The SB ACC is considered part of the ACC at the zero meridian (Klatt et al., 2005). The zone between the PF and the SB ACC is known as the Antarctic Zone (AAZ). South of the ACC the sub-polar cyclonic Weddell Gyre is found. The Weddell Front is the northern boundary of the Weddell Gyre and was observed by Klatt et al. (2005) at 56°22′30″S during previous expeditions between 1996 and 2001. The stations in the South East Atlantic Ocean, except the most northerly one (see text Section 3.2.), and the stations in the Bouvet triple junction region (see text Section 3.3.) were within the ACC. The stations in the deep Weddell Basin (see text Section 3.4.) were south of 56°22′30″S and therefore in the Weddell Gyre.

Along the transect several major water masses were sampled, which are described in Whitworth and Nowlin (1987) and briefly summarised here (Fig. 2). Between the Subtropical Front and the SAF the Subantarctic Surface Water (SSW) is found above the salinity minimum of the Antarctic Intermediate Water (AAIW). The transition surface waters between the SAF and the PF are marked by a steady decrease in temperature and salinity, and in this paper are considered to be part of the Subantarctic Surface Water. South of the PF, in the Antarctic Zone and Weddell Gyre, the cold ($\theta < 5$ °C) Antarctic Surface Water (AASW) constitutes the upper water layer. The Winter Water (WW) is the even colder water layer that shows as a temperature minimum at the bottom of the AASW. The Winter Water is a remnant from the last winter before the overlying water was warmed by the summer. In the deep South Atlantic Ocean the relatively saline North Atlantic Deep Water (NADW) that flows in from the north is found, underlain by the cold Antarctic Bottom Water that flows northward. The Antarctic Intermediate Water is relatively fresh (compared to NADW) and sinks in between the Subantarctic Surface Water and NADW at the SAF and flows northward. Within the ACC (between the SAF and the Weddell Front) the most extensive water mass is the Circumpolar Deep Water, which is commonly distinguished between Upper Circumpolar Deep Water (UCDW) and Lower Circumpolar Deep Water (LCDW). The Upper Circumpolar Deep Water has a relative temperature maximum induced by the colder overlying Antarctic Intermediate Water and Winter Water. The LCDW has a salinity maximum due to the influence from the relatively warm, saline NADW from the north (Figs. 2 and 4). The deeper parts of the LCDW receive influence from

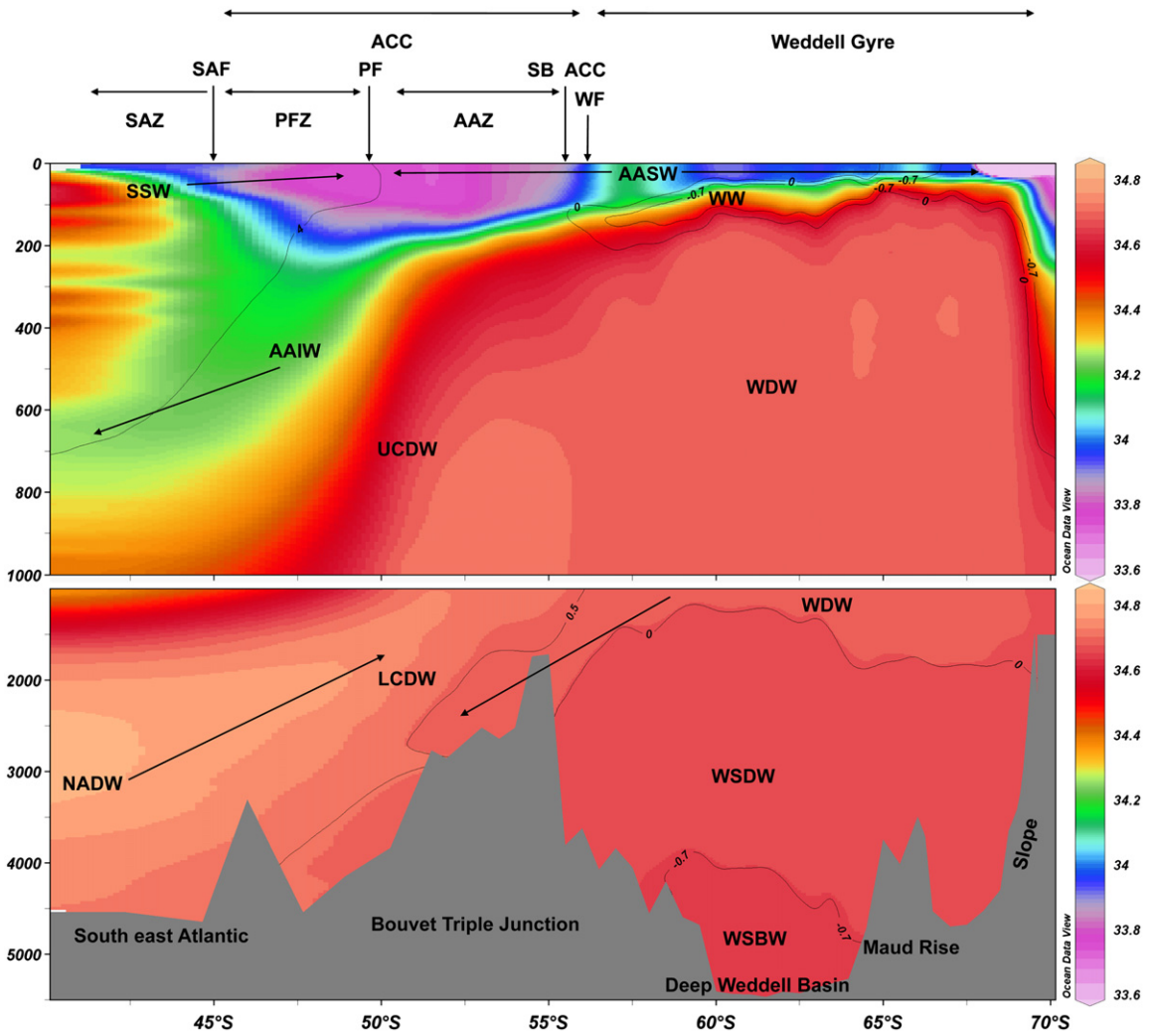

Fig. 2. Water masses and fronts along the entire transect (see Fig. 1). Salinity is represented in colour scale and isobars represent the potential temperature (°C). Upper panel shows the upper 1000 m; the lower panel the remainder of the water column. Abbreviations in alphabetical order: AAIW: Antarctic Intermediate Water (salinity minimum); AASW: Antarctic Surface Water (salinity < 34.6); AAZ: Antarctic Zone; ACC: Antarctic Circumpolar Current; LCDW: Lower Circumpolar Deep Water (salinity maximum); NADW: North Atlantic Deep Water (salinity maximum); PF: Polar Front; PFZ: Polar Frontal Zone; SAF: Sub-Antarctic Front; SAZ: Sub-Antarctic Zone; SB ACC: Southern Boundary of the Antarctic Circumpolar Current; SSW: Subantarctic Surface Water ($\theta > 4$ °C); UCDW: Upper Circumpolar Deep Water (salinity > 34.4); WDW: Warm Deep Water ($\theta > 0$ °C, salinity > 34.6); WF: Weddell Front; WSBW: Weddell Sea Bottom Water ($\theta < 0.7$ °C); WSDW: Weddell Sea Deep Water (-0.7 °C $< \theta <$ 0.0 °C); and WW: Winter Water (θ minimum).

the colder, less saline Weddell Sea Deep Water (WSDW) from the south. Along the slope of the Bouvet triple junction region (see text Section 3.3.), the influence of this WSDW can be clearly seen in lower potential temperatures ($\theta < 0.5$ °C) (Fig. 2).

In the deep Weddell Basin, below the AASW and Winter Water, the Warm Deep Water (WDW) is found, which is largely replenished by LCDW (Klatt et al., 2005). Underlying the WDW is the Weddell Sea Deep Water (WSDW), which is more saline and has a lower potential temperature (-0.7 °C $< \theta <$ 0.0 °C). Even colder ($\theta < -0.7$ °C) is the deepest water layer, the Weddell Sea Bottom Water (WSBW) formed at the surface close to the Antarctic continent in winter by cooling and brine rejection due to sea ice formation. The WSDW is believed to be formed by mixing between WDW and WSBW, but there is also evidence that WSDW is formed directly from surface waters and modified WDW (Klatt et al., 2005 and references therein).

3.2. South East Atlantic Ocean

In the South East Atlantic Ocean four stations were sampled for Al (Fig. 3), of which one in the Sub-Antarctic Zone (42°20′S, 9°E), two in the Polar Frontal Zone (46°S, 5°53′E and 47°40′S, 4°17′E) and one just south of the PF in the Antarctic Zone (50°16′S, 1°27′E). In the Subantarctic Surface Water in the SAZ (42°20′S, 9°E), the concentrations of Al were below 1 nM until 250 m depth with a minimum of 0.48 at 250 m (Fig. 4A). From 300 m depth downward, values were considerably higher with a maximum of 2.35 nM coinciding with the salinity minimum of the Antarctic Intermediate Water at 500 m depth (Fig. 4A). Below this maximum, concentrations of Al were around 1.6 nM until about 1750 m depth followed by a steep increase into the NADW with values over 6 nM at the salinity maximum at about 3000 m depth (Fig. 4A). Below this maximum the Al values remained around 6 nM. At the two stations in the Polar Frontal Zone, the concentrations in the Subantarctic Surface Water were around 1 nM. Concentrations decreased to subsurface minima of 0.23 nM at 150 m and 0.32 nM at 100 m depth at 46°S, 5°53′E and 47°40′S, 4°17′E, respectively. At both stations a maximum in the concentrations of Al (4 and 2.65 nM, respectively) was observed in the Lower Circumpolar Deep Water, which coincided with the salinity maximum of the NADW influence at about 2000 m (Fig. 4B and C). The station just south of the PF (50°16′S, 1°27′E) was located at

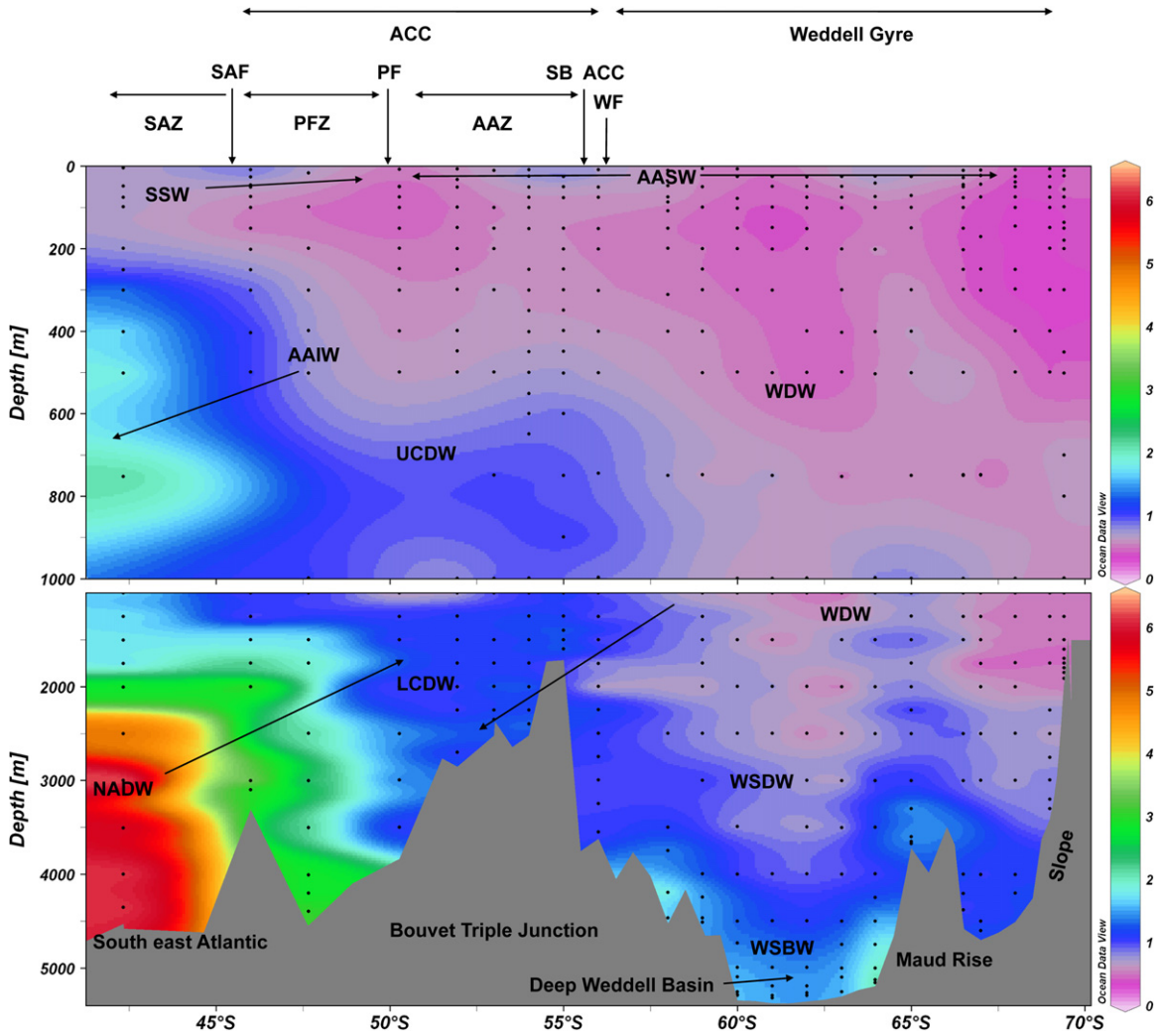

Fig. 3. Concentrations of dissolved Al (nM) over the entire water column at all 22 TM stations along the zero meridian and in the South East Atlantic Ocean. Upper panel shows the upper 1000 m; the lower panel the remainder of the water column. Of the 487 samples analysed for Al, 41 samples (8.4%) were suspected outliers and therefore not further used in the figures. Abbreviations in alphabetical order: AAIW: Antarctic Intermediate Water; AASW: Antarctic Surface Water; AAZ: Antarctic Zone; ACC: Antarctic Circumpolar Current; LCDW: Lower Circumpolar Deep Water; NADW: North Atlantic Deep Water; PF: Polar Front; PFZ: Polar Frontal Zone; SAF: Sub-Antarctic Front; SAZ: Sub Antarctic Zone; SB ACC: Southern Boundary of the Antarctic Circumpolar Current; SSW: Subantarctic Surface Water; UCDW: Upper Circumpolar Deep Water; WDW: Warm Deep Water; WF: Weddell Front; WSBW: Weddell Sea Bottom Water; and WSDW: Weddell Sea Deep Water.

the onset of the flank of the Bouvet triple junction region. The concentrations at this station over the entire water column were lower than at the stations north of the PF and no coinciding maxima of Al and salinity were observed. Concentrations in the upper 500 m were below 0.5 nM and like north of the PF, a subsurface minimum was observed at 150 m depth (of 0.19 nM). Below 500 m depth the concentrations of Al increased with depth to a maximum of 1.44 nM at 2500 m depth, followed by a slight decrease to 1 nM at the greatest sampled depth (Fig. 3).

3.3. *Bouvet triple junction region*

The region where the southernmost segment of the Mid-Atlantic Ridge, the westernmost segment of the Southwest Indian Ridge and the easternmost segment of the American-Antarctic Ridge meet is referred to as the Bouvet triple junction region, hereafter called Bouvet region (Ligi et al., 1999). Five stations were sampled with 1° resolution at every full degree latitude along the zero meridian in this Bouvet region (Fig. 5), of which four in the Antarctic Zone (51°57′S, 53°S, 54°S and 55°S) and one between the southern boundary of the ACC and the Weddell Front (56°S). Concentrations of Al were low (<0.5 nM) in the AASW at 51°57′S and a subsurface minimum of 0.25 nM was observed at 250 m depth. Concentrations of Al in the AASW increased in a southwards direction with concentrations of 0.56, 1.53 and 1.78 nM Al at 53°S, 54°S and 55°S, respectively. Subsurface minima of about 0.5 nM Al were observed at these three stations between 100 and 200 m depth. South of the southern boundary of the ACC, surface concentrations of Al were lower again, around 0.8 nM in the upper 25 m and a subsurface minimum of 0.37 nM was observed at 200 m depth. A similar trend of higher concentrations over the shallow part and lower concentrations over the deep part of the Bouvet region was observed in the Circumpolar Deep Water (Fig. 5). Concentrations were around 1 nM in the deep LCDW at 51°57′S and about 1.4 nM in the deep LCDW at 53°S and 54°S. At the shallowest station (55°S) of 1600 m depth, the concentration was about 1.4 nM below 1000 m depth, which is very similar to the deeper concentration in the LCDW observed at 53°S and 54°S. South of the southern boundary of the ACC, concentrations of Al were lower again, around 0.7 nM in the WDW and around 1 nM in the WSDW. Overall, in the shallowest part of the Bouvet region the concentrations of Al were elevated in the surface and the deepest layer, and concentrations decreased away from the triple junction ridge.

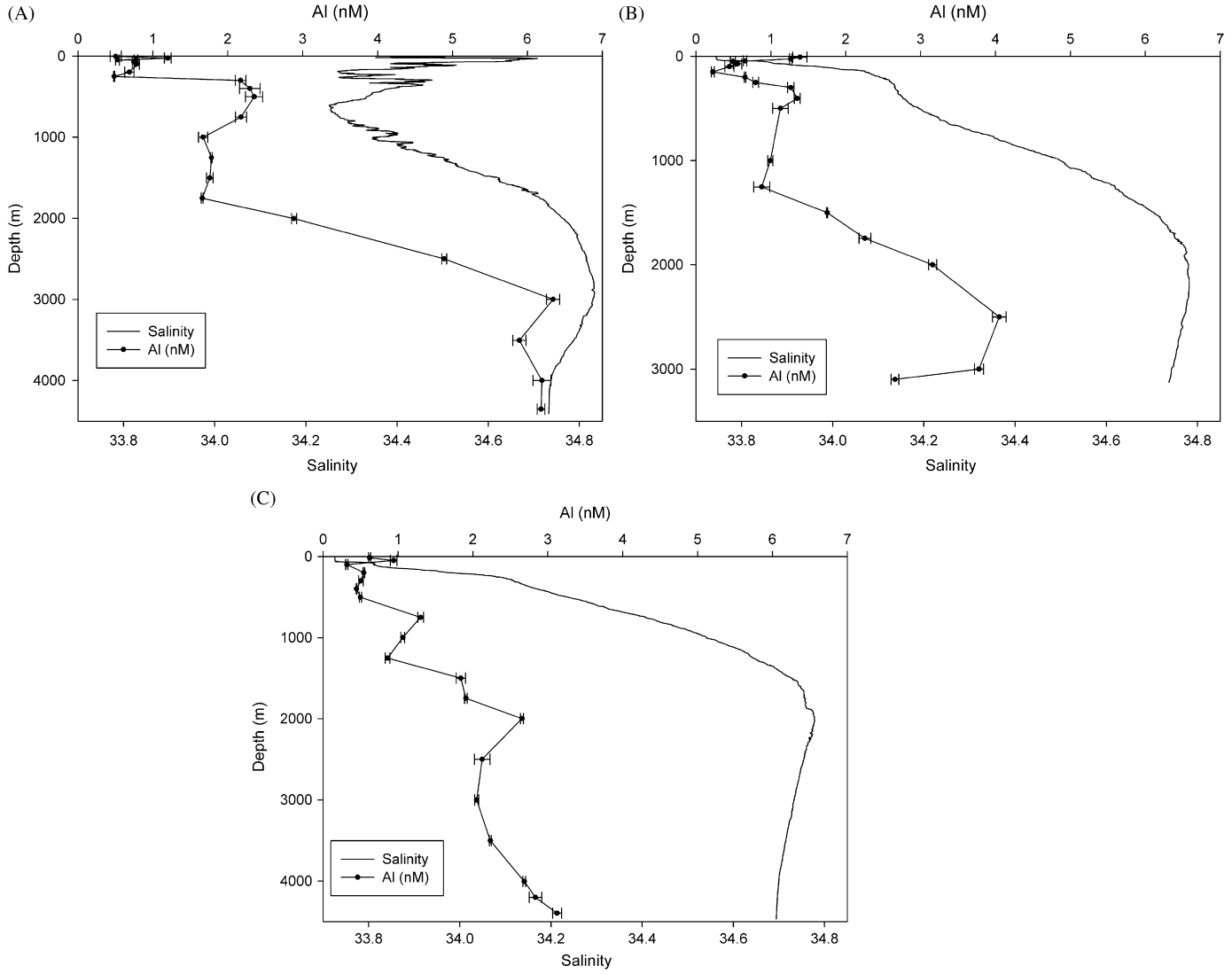

Fig. 4. (A) Profiles of dissolved Al (nM) (filled circles) and salinity over depth at the most northerly TM station (42°20′S, 9°E) in the SAZ in the South East Atlantic Ocean. Error bars represent standard deviation of triplicate analysis. ((B) Profiles of dissolved Al (nM) (filled circles) and salinity over depth at the most northerly of the two TM stations in the PFZ (46°S, 5°53′E) in the South East Atlantic Ocean. Error bars represent standard deviation of triplicate analysis. Of the 21 samples analysed for Al, 1 sample was a suspected outlier and therefore not further used in the figure. (C) Profiles of dissolved Al (nM) (filled circles) and salinity over depth at the most southerly of the two TM stations in the PFZ (47°40′S, 4°17′E) in the South East Atlantic Ocean. Error bars represent standard deviation of triplicate analysis.

3.4. Deep Weddell Basin

South of the Bouvet region the zero meridian transect crosses the deep Weddell Basin towards the Antarctic continental slope to the edge of the continental ice-sheet at approximately 69°30′S. Twelve stations were sampled with 1° resolution at every full degree latitude (except 1 station at 66°30′S instead of 66°S) and the southernmost station was as close to the edge of the continental ice-sheet as possible at 69°24′S (Fig. 5).

Two stations were sampled between the Bouvet region and the deepest part of the Weddell Basin. In the AASW the concentrations were about 0.6 nM Al at the surface, followed by a subsurface minima of 0.39 and 0.3 nM around 100 m depth at 58°S and 59°S, respectively. Concentrations of Al increased slightly with increase in depth to about 0.7 nM in the WDW at both stations. At 58°S, concentrations of Al increased to about 2 nM in the WSDW, which was a higher concentration than observed in the deepest layer over the Bouvet region. At the station at 59°S, concentrations of Al increased into the WSDW to a maximum of only 0.88 nM and in the WSBW, concentrations increased to 1.56 nM Al.

In the deepest part of the Weddell Basin five stations (60°S, 61°S, 62°S, 63°S and 63°58′S) were sampled with maximum sampled depths of around 5200 m. In the AASW of the two more northerly stations, low concentrations of Al around 0.3 nM were observed in the upper surface, overlying a minimum of about 0.2 nM between 100 and 150 m depth. Southwards, the concentrations of Al in the upper surface increased from 0.5 nM, to 0.8 and 1.4 nM Al, respectively. Subsurface minima in the concentrations of Al of 0.34, 0.28 and 0.57 nM were observed around 100 m depth at these three stations. Below the Al minima, the concentrations of Al varied somewhat in the deeper part of the Weddell Basin, but gradually increased with depth until remarkably similar values at 4000 m depth of 0.79, 0.77, 0.81, 0.83 and 0.98 nM, respectively, from north to south. Deeper than 4000 m the concentrations of Al increased to a maximum of around 1.5 nM close to the sediments in the WSBW, except for the most southerly station in this deep part of the Weddell Basin. At this station the concentration increased to a maximum of 2.79 nM in the WSBW at the greatest sampled depth of 5150 m.

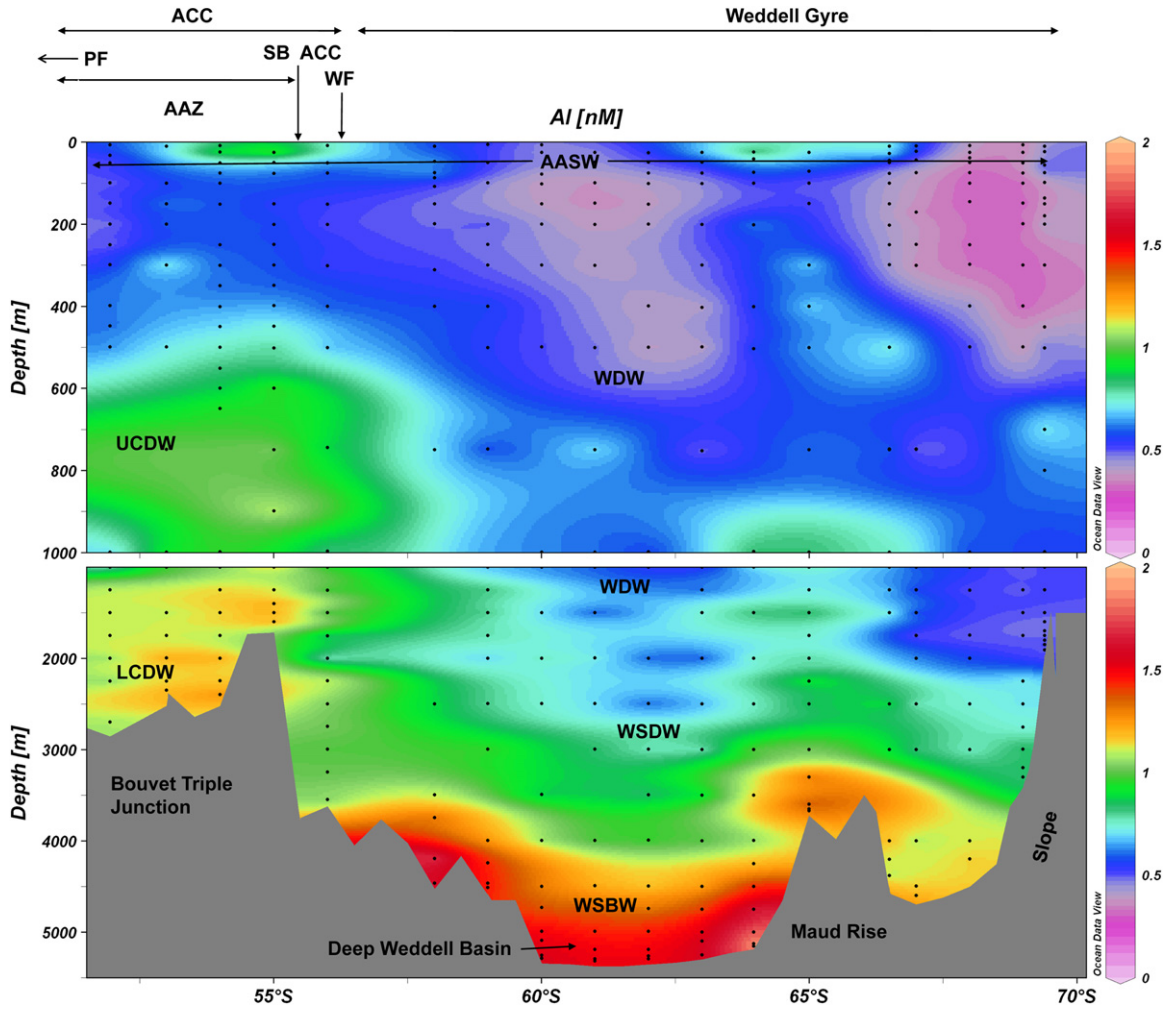

Fig. 5. Concentrations of dissolved Al (nM) over the entire water column at 18 TM stations in the Bouvet triple junction ridge region and the deep Weddell Basin. Upper panel shows the upper 1000 m; the lower panel the remainder of the water column. Note the different colour scale compared to Fig. 3. Of the 401 samples analysed for Al, 36 samples (9%) were suspected outliers and therefore not further used in the figures. Abbreviations in alphabetical order: AASW: Antarctic Surface Water; AAZ: Antarctic Zone; ACC: Antarctic Circumpolar Current; LCDW: Lower Circumpolar Deep Water; PF: Polar Front; SB ACC: Southern Boundary of the Antarctic Circumpolar Current; UCDW: Upper Circumpolar Deep Water; WDW: Warm Deep Water; WF: Weddell Front; WSBW: Weddell Sea Bottom Water; and WSDW: Weddell Sea Deep Water.

Further south the basin is less deep (3700 m) on the flank of Maud Rise where one station was sampled at 65°S, followed by three more deep (4500 m) stations at 66°30′S, 67°S and 68°S (Fig. 5). Surface concentrations of Al in the AASW decreased from 0.56 to 1.3 nM, over and just south of the flank of Maud Rise, to just below 0.4 nM at the two stations further south. Below the subsurface minima that were observed around 75 m depth (0.37, 0.30, 0.22 and 0.16 nM from north to south), the concentrations increased with increasing depth. At the station near Maud Rise the concentrations were elevated in WSDW with a maximum of 1.75 nM at 3600 m depth. In comparison, the concentrations of Al were only around 0.8 nM at 4000 m in the WSDW in the deepest part of the Weddell Basin and around 1.3 nM in the deepest part of the WSDW south of Maud Rise. A similar enrichment of Al was observed over the sea floor rise of the Bouvet region, indicating that the bottom topography has an influence on the deep distribution of Al.

The two most southerly stations of the zero meridian transect (69°S and 69°24′S) were sampled over the Antarctic continental slope. The shallowest station (69°24′S) was as close to the edge of the continental ice-sheet as possible, but given the depth, obviously not yet on the continental shelf (Fig. 5). Surface concentrations of Al in the AASW increased from 0.15 nM at 69°S to 0.62 nM near the continental ice edge. Below the subsurface minimum of 0.10 nM observed at 75 m depth at 69°S, concentrations of Al increased with increasing depth to 0.81 nM at the greatest sampled depth of 3300 m. This concentration of Al is similar to the concentrations observed at similar depth in the deeper basin. At the ice edge station, concentrations of Al below the subsurface minimum (0.35 nM at 100 m depth) varied between ~0.4 and 0.6 nM. At the greatest sampled depth (1900 m) the concentration of Al was 0.44 nM, which is a similar concentration as found at comparable depth in the deep basin.

3.5. Surface layer

The concentrations of Al in the upper 25 m of the surface layer were quite patchy (Fig. 6A). Nevertheless, most concentrations were between 0.25 and 0.65 nM, but some extreme values of up to 1.8 nM were observed. Deeper than the relatively high surface values, usually an Al subsurface minimum was observed at an average depth of approximately 120 m with an average concentration of Al of 0.33 nM (S.D.=0.13 nM; n=22). The concentration of Al in the subsurface minimum followed the average concentration of Al in the part of the water column above the observed subsurface minimum (i.e. average of all concentrations of Al shallower than the depth of the subsurface minimum at a station) quite well (Fig. 6A). However, the peaks in the concentrations of

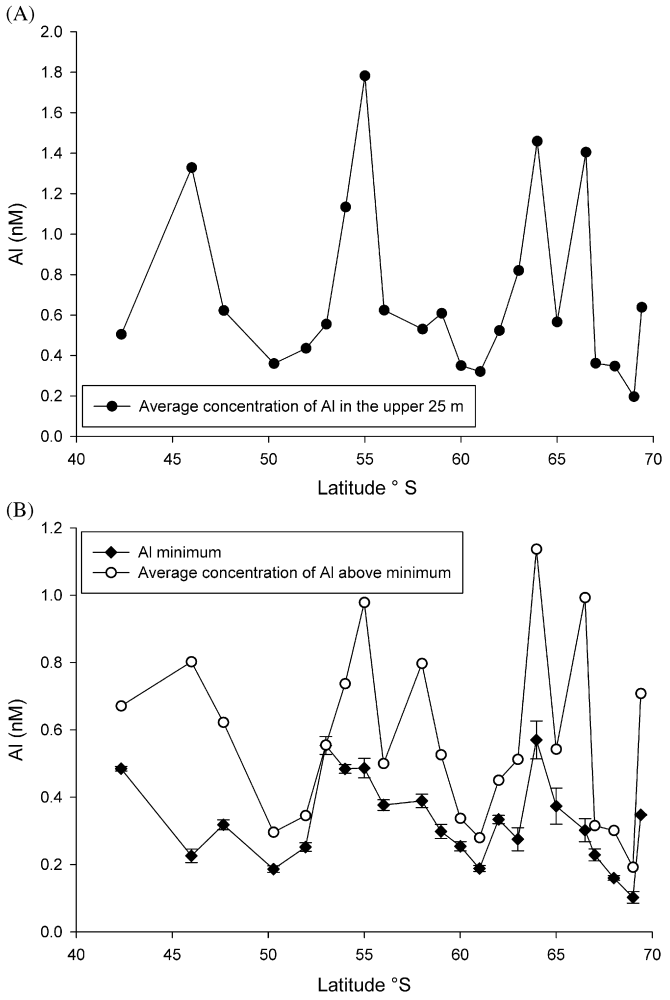

Fig. 6. (A) Average concentrations of dissolved Al (nM) in the upper 25 m of the water column versus latitude along the transect at all 22 stations. The concentration of Al is an average of two depths (typically 10 and 25 m) in the upper 25 m, which is within the upper mixed layer at all stations. (b) Concentrations of dissolved Al (nM) at the Al subsurface minimum (filled diamonds) and average concentrations of dissolved Al (nM) above the latter minimum (open circles) (i.e. average of all concentrations of Al shallower than the depth of the subsurface minimum at a station) versus latitude along the transect at all 22 stations. Error bars represent standard deviation of triplicate analysis.

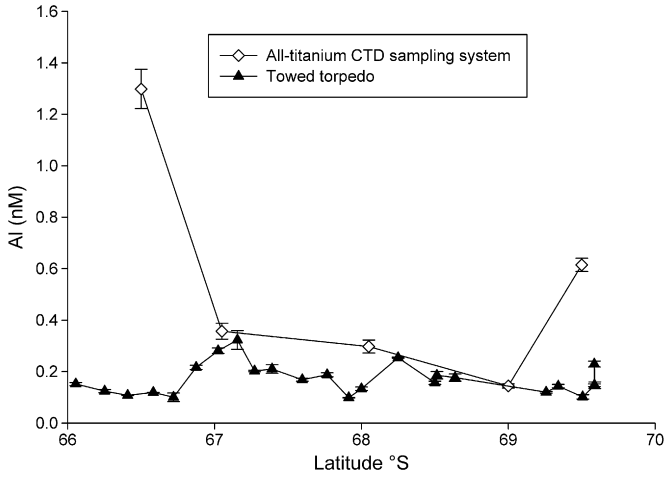

Fig. 7. Concentrations of Al (nM) in the upper surface layer sampled with the towed torpedo (filled triangles) and with the all-titanium CTD sampling system (open diamonds) versus latitude south of 66°S. Error bars represent standard deviation of triplicate analysis.

Al in the subsurface minimum are less extreme than the peaks in the water column shallower than the subsurface minimum. This shows that elevated surface concentrations affect the underlying water column, but that this effect fades away with depth, most likely due to (scavenging) removal of Al.

The samples collected using the torpedo south of 66°01′S (see text Section 2.1.) gave results of around 0.20 nM Al, which was lower at some stations as compared to the samples from the all-titanium sampling CTD system (Fig. 7). The high surface values found at 66°30′S sampled from the all-titanium sampling CTD system were not confirmed by samples from the torpedo in the transit to and from this station. However, at the same station the concentration of dissolved Mn sampled by the CTD system was also enriched (Middag et al., 2011) and shipboard underway salinity at 5 m depth showed a decrease from a salinity of 34.1 at 66°28′S to a salinity of 33.9 at 66°32′S (not shown). This drop in salinity was also confirmed by the CTD sampling system, with a salinity of 33.9 at 66°30′S compared to 34.1 and 34.0 at the CTD stations north and southwards of 66°30′S. This indicates that surface enrichments due to melting of sea-ice or the land-ice edge or a derived iceberg can be a very local phenomenon. The difference between the samples from the torpedo and the CTD sampling system could potentially be explained by the sampling method. The samples from the CTD sampling system were taken even under conditions of floating ice and near icebergs, whereas the torpedo could only be deployed under ice-free conditions to avoid damage or loss of equipment. Therefore, elevated concentrations due to ice melt are likely to be missed by the torpedo sampling.

The torpedo data shows, like the all-titanium CTD sampling system data, that concentrations of Al were slightly elevated at the edge of the ice-sheet, yet in fact the lowest just north of the edge of the continental ice-sheet. Combined with the localised Al enrichments in the top of the AASW this indicates that the edge of the continental ice-sheet is not the most important source of Al. Most likely both direct atmospheric input and indirect atmospheric input via dust particles entrained in melting ice influence the distribution of Al in the surface layer, which can therefore be quite patchy in regions with intense local icebergs and ice melting.

4. Discussion

4.1. Comparison with previously reported Al data of the Southern Ocean

The complete section (Fig. 3), including the torpedo data, is the first comprehensive dataset (470 data points) of dissolved Al in the Southern Ocean. Previously, Moran et al. (1992) collected unfiltered seawater and reported concentrations of Al ranging from 1.1 to 3.1 nM below 1000 m depth (in the WDW and WSDW) in the central Weddell Gyre. The reported precision of about ± 0.5 nM, blank of 1 nM and detection limit of 1–1.5 nM are in the range of the 0.2–1.5 nM of our dissolved Al values (in the central Weddell Gyre WDW and WSDW), precluding comparison between the two datasets.

Van Bennekom et al. (1991) collected unfiltered samples in the Weddell–Scotia Confluence and used the same method as Moran et al. (1992). Similarly, the precision (0.3 nM) and the blank (0.8 nM) would preclude comparison with the low dissolved concentrations reported here. Nevertheless, when disregarding the concentration differences and merely looking at the shape of

vertical profiles, similarities are clear between the Scotia Ridge and Weddell Sea profiles reported by Van Bennekom et al. (1991) and this study. The Weddell Sea profile did show a subsurface minimum, followed by an increase with depth. The Scotia Ridge profile had been sampled with less resolution in the upper water column but also a decrease with increase in depth from elevated surface values was visible. Moreover, an increase near the top of this Scotia Ridge had been observed, just as observed here over the ridge of the Bouvet region.

Van Beusekom et al. (1997) collected unfiltered seawater in the Enderby and Crozet Basins near the Kerguelen plateau, at about 60°E. Occasionally bottom water samples were filtered. The detection limit of the Al determination was 0.24 nM. Their most southerly station at 52°S in the ACC shows good consistency with the data from this study. At their station the concentration of Al decreases from 0.76 nM near the surface to about 0.4 nM between 500 and 1000 m depth followed by an increase with depth with the highest value of 1.19 nM at 4400 m (Van Beusekom et al., 1997). At our station just north of the Bouvet region (50°16′S, 1°27′E, Fig. 3), hence beyond the profound influence from the NADW (see text Section 3.2.), the surface concentrations were somewhat lower, but deep water values are in good agreement.

A model using surface concentrations of Al combined with a global chemical element cycling ocean model and a global dust entrainment and deposition model has been constructed to constrain dust deposition to the oceans (Han et al., 2008). For the Southern Ocean the mean concentrations of Al in the surface ocean (0–50 m) and the subsurface ocean (150–500 m) are reported as the averages of previous measurements in the Southern Ocean and the results of the model (Han et al., 2008 and references therein). For the surface ocean of the Southern Ocean the average of previous observations was 2.23 nM Al and the average modelled value is 1.44 nM. The average concentration of Al in the upper 50 m of all 22 stations in this study is 0.62 nM (S.D.=0.30 nM), which is considerably lower than both the previous observations and the model output. For the subsurface of the Southern Ocean the average of previous observations was 2.38 nM and the modelled value was 0.9 nM. The average concentration of Al in the 150–500 m depth interval of all 22 stations from this study is 0.55 nM (S.D.=0.30 nM), which is again considerably lower than both the previous observations and the model output. Nevertheless, in contrast to the average of the previous observations, the model predicted lower values of Al in the subsurface compared to the surface of the Southern Ocean, which is a trend that is confirmed at least qualitatively by the current data. It should be noted though that the difference between the average concentration of Al of the surface layer and the average concentration of Al of the subsurface layer is not significant due to the large standard deviation associated with the spatial variability along the transect. Nevertheless, further refinement of the global simulation model is now feasible towards better mimicking the true concentrations of Al.

4.2. Surface distribution

The distribution of Al in the upper water column to about 200–250 m depth shows elevated surface concentrations followed by a subsurface minimum (see text Section 3.5.). The average concentration of Al in the upper 25 m of all 22 stations is 0.71 nM (S.D.=0.43 nM), but there is a quite large variability, represented in the large standard deviation and also shown in Fig. 6A. When ignoring all concentrations of Al in the upper 25 m above 1 nM (5 out of 22 values) the average concentration is less at 0.5 nM (S.D.=0.15 nM), with a much smaller standard deviation. Thus the background concentration of Al in this region is approximately 0.5 nM and the large deviations suggest that distinct local inputs of either sea ice or atmospheric dust must be of importance. Even though the surface concentrations of Al are elevated, they are lower than most reported concentrations in other oceanic regions with known low dust input. Surface concentrations reported for ocean regions with high dust input such as the North Atlantic Ocean or Mediterranean Sea (i.e. Kramer et al.. 2004; Measures, 1995; Chou and Wollast, 1997) are much higher and can be up to 96 nM (Hydes et al., 1988) in the Mediterranean Sea. Moreover in comparison with the concentrations of Al in surface waters of the Southern Ocean, the average surface concentrations of Al in the upper 25 m of the ice covered Arctic Ocean are considerably higher at 0.98 nM (n=56 S.D.=0.3 nM) (Middag et al., 2009). In the Pacific Ocean elevated surface concentrations (followed by mid-depth minimum) are usually observed (e.g. Orians and Bruland, 1986; Bruland et al., 1994; Measures et al., 2005) and range between 0.3 and 8 nM. However in the subarctic gyre of the North Pacific Ocean, Measures et al. (2005) reported concentrations of Al in samples of the surface water as low as <0.1 nM collected by a towed torpedo, but in the collected vertical profiles the surface values of Al were higher at $\sim$1 nM (Measures et al., 2005). Similarly, the concentrations of Al from the towed torpedo samples (target depth of 1.5 m) were also sometimes lower (see text Section 3.5.) compared to the concentrations from the shallowest sampled depth (usually about 10 m depth) with the all-titanium CTD sampling system.

Besides the variability in the surface concentrations, the observed subsurface minimum of Al of 0.33 nM (n=22; S.D.=0.13 nM) around 120 m depth and the relation between the subsurface minimum and the surface concentrations indicate a surface source (see text Section 3.5.). The concentrations of Al in the surface layer and in the underlying Al minimum (Fig. 6B) do not show an unambiguous trend of increasing concentrations towards the edge of the continental ice-sheet. The concentrations were elevated at the edge of the continental ice-sheet, but the lowest concentrations were actually found just north of this continental ice edge. This indicates that melting of this 'continental' ice was a source of Al, but apparently not over long distances. Atmospheric dust input is another source of Al to the surface layer, but dust input to the Southern Ocean is known to be very little (e.g. Duce and Tindale, 1991; Han et al., 2008). Furthermore, in a perennial ice covered ocean like the southern part of the Southern Ocean, the direct dust deposition is likely to be highly variable in place and time. When the sea ice melts pulses of trace metals into the surface waters can be expected (Measures, 1999). The patchy distribution of Al in the surface layer of especially the Weddell Gyre matches what one would expect from influence of melting sea ice and icebergs, releasing the accumulated trace metals locally. In the surface waters over the Bouvet region at 54°S and 55°S the concentrations of dissolved Al, dissolved Mn (Middag et al., 2011) and dissolved Fe (Klunder et al., 2011) were elevated over a band of more than 2° latitude. This is consistent with direct atmospheric dust input (either dry (aeolian) or wet (precipitation) dust deposition) due to the larger scale and the quite northerly location. This was confirmed by Klunder et al. (2011) based on air mass back-trajectories using the NOAA HYSPLIT model. In the perennial ice covered Weddell Gyre the concentrations of Mn are all extremely depleted by primary production in the surface (Middag et al., 2011) and do not show a link with concentrations of Al, except for the station at 66°30′ S (see text Section 3.5.). Similarly, no strong relation was observed between the concentrations of Al and Fe in the Weddell Gyre. Presumably the strong biological function, hence uptake of Mn and Fe, obscures the likely underlying correlations with Al due to a common dust input source.

4.3. Intermediate and deep distribution

Below the Al subsurface minimum the concentrations of Al showed an increasing trend with depth. This increase is most profound in the South East Atlantic Ocean part of the transect due to the NADW (see text Section 3.2. and Fig. 4). This water mass has relatively high concentrations of Al (Moran and Moore, 1991). Over the relatively shallow Bouvet region the concentrations of Al increased with depth to values higher than 1 nM at approximately 1000 m depth and to about 1.4 nM in the deepest part of the water column (Fig. 5). These concentrations are lower than observed at similar depths in the South East Atlantic Ocean (Fig. 3), but considerably higher than at similar depths in the Weddell Basin (Fig. 3). The shallow end of the LCDW is influenced by the NADW (see text Section 3.1.), explaining the elevated concentrations of Al below 1000 m depth. However, the deep end of the LCDW receives influence from the WSDW that has much lower concentrations of Al (<1 nM). If only conservative mixing was of importance for the distribution of Al over the Bouvet region, lower concentrations of Al would have been observed in the deep end of the LCDW compared to the shallow end of the LCDW (Fig. 2). In contrast higher concentrations of Al were observed (see text Section 3.3. and Fig. 5), indicating another source of Al for the deep end of the LCDW. In the Weddell Basin at the flank of Maud Rise elevated concentrations of Al compared to similar depths elsewhere in the basin were observed (see text Section 3.4. and Fig. 5). The apparent influence of these sea floor elevations on deep Al has to come from the sediments, as the water masses around have lower concentrations of Al. Perhaps sediments get resuspended at these sea floor elevations by passing currents that subsequently increase the concentration of Al in the water by partial dissolution. At the flank of Maud Rise, the concentrations of Mn were also slightly elevated near the sediments (Middag et al., 2011), further indicating the elevated concentrations of Al could indeed have a sedimentary source. Furthermore, the light transmission and concentrations of oxygen decreased close to the sediments, indicating some sediment resuspension. However, the decrease of light transmission and concentrations of oxygen close to the sediments was also observed at most other stations and not specifically or more profoundly at the stations near sea floor elevations. Another possible explanation is a diffusive flux of Al from the sediments as suggested by Van Beusekom et al. (1997), but based on the presented data there is no reason to assume this process has more effect near sea floor elevations.

In the WSBW the concentrations of Al were higher compared to the overlying WSDW and to the deepest water layers over Maud Rise and the Bouvet region (see text Section 3.4.) as was also seen for Mn (Middag et al., 2011). The WSBW is formed at the surface close to the Antarctic continent in winter by cooling and brine rejection due to sea ice formation and subsequent sinking along the slope to the deepest part of the Weddell Basin (see text Section 3.1.). The concentrations of dissolved Al were generally quite low in the surface of the Southern Ocean when there is no significant dust input or other surface source. The recent contact with the atmosphere, ice and continental shelf sediments in combination with scavenging and biological uptake undoubtedly enriched the water near the Antarctic continent in trace metal rich particles. When the forming WSBW sinks down the slope, particles are broken down microbially and thereby releasing the Al into solution, perhaps aided by the pressure dependent solubility of Al (Moore and Millward, 1984). Besides this, sedimentary particles are most likely getting suspended when the forming WSBW is cascading down the continental slope. These suspended particles can partly dissolve and also release Al into solution (Moran and Moore, 1991). Due to microbial breakdown and mixing with deep water with lower concentrations of particles, the scavenging intensity decreases with deep slope convection. A lower particle concentration means a lower scavenging rate for Al, which aids the dissolution of Al from the Al-rich particles, in addition to the presumed pressure-dependent solubility.

Elevated concentrations of Al in the deep basin have also been observed and related to slope ventilation processes in the Arctic Ocean (Middag et al., 2009) and Norwegian Sea (Measures and Edmond, 1992). Deep water formation due to cooling and brine rejection by sea ice formation appears to be an important factor in the distribution of Al in the global deep ocean.

4.4. Living apart and together in the modern ocean: cycling of Al and Si

In the oceans the distribution of Al appears to be partly linked to the Si cycle through the incorporation of Al in biogenic silica and/or preferential scavenging of Al onto biogenic siliceous particles (e.g. Van Bennekom et al., 1991, 1997; Gehlen et al., 2002; Han et al., 2008; Middag et al., 2009). This shows the clear correlations that have been found between dissolved Al and Si in the Mediterranean Sea (Hydes et al., 1988; Chou and Wollast, 1997), the North Atlantic Ocean (Kramer et al., 2004) and the Arctic Ocean (Middag et al., 2009). In contrast, in the Pacific Ocean and Indian Ocean these correlations have, to the best of our knowledge, not been observed. In Fig. 8A, the concentrations of Al have been plotted versus the concentrations of Si for the Southern Ocean, and in Fig. 8B for the Mediterranean Sea, North East Atlantic Ocean and Arctic Ocean. In the Southern Ocean no correlation between Al and Si was observed with the exception of a trend in the NADW (Fig. 8A and see text below). Here we will propose our concept to explain the coupled and uncoupled cycling of Al and Si based on the observations in the Southern Ocean and in other ocean regions.

In the North East Atlantic Ocean the slope of the Al–Si relation observed in the North Atlantic Central Water (NACW) was 1.9×10^{-3} (Fig. 8C), comparable to the slope of the Al–Si relation in the Atlantic and Intermediate Depth Water (AIDW) of 2.2×10^{-3} in the Arctic Ocean (Middag et al., 2009). The slope of $\sim2\times10^{-3}$ of the Al–Si relation in the subsurface waters of the NACW and AIDW is deemed consistent with the concept of diatoms in the surface waters accumulating Al and Si in that same ratio (Middag et al. 2009). Upon export of diatom particles into underlying subsurface waters the siliceous diatom frustules dissolve with the same ratio, thus imprinting the Al:Si ratio of biogenic silica in the dissolved Al/Si ratio (derived from the slope of the Al–Si relation). However, this mechanism can be obscured by additional Al input like deep slope convection with partly dissolving sediment particles or very high input of atmospheric dust, resulting in the much steeper slopes of around 10×10^{-3} in the deep Arctic Ocean and the Mediterranean Sea (Middag et al., 2009). Given the average crustal abundance ratio Al:Si$=\sim$1:3 one realises that even a modest lithogenic terrigenous input of Si is accompanied by a relatively massive input of Al leading to a much higher value of $\sim10\times10^{-3}$ as the slope of the Al–Si relation.

The relationship can also be distorted in opposite direction by very low supply of Al like in the Southern Ocean or Pacific Ocean where no apparent Al–Si relation is observed. In this case virtually the entire limited available Al is depleted in the surface layer, resulting in only minor additions of Al in the deeper water layers by the dissolution of the formed biogenic silica. The limited availability of Al in the Southern Ocean also shows in the lower Al/Si ratio in biogenic silica of natural assemblages of Antarctic diatoms of 0.033×10^{-3} (Collier and Edmond, 1984) compared to observations in the Arctic Ocean with a ratio in the order of

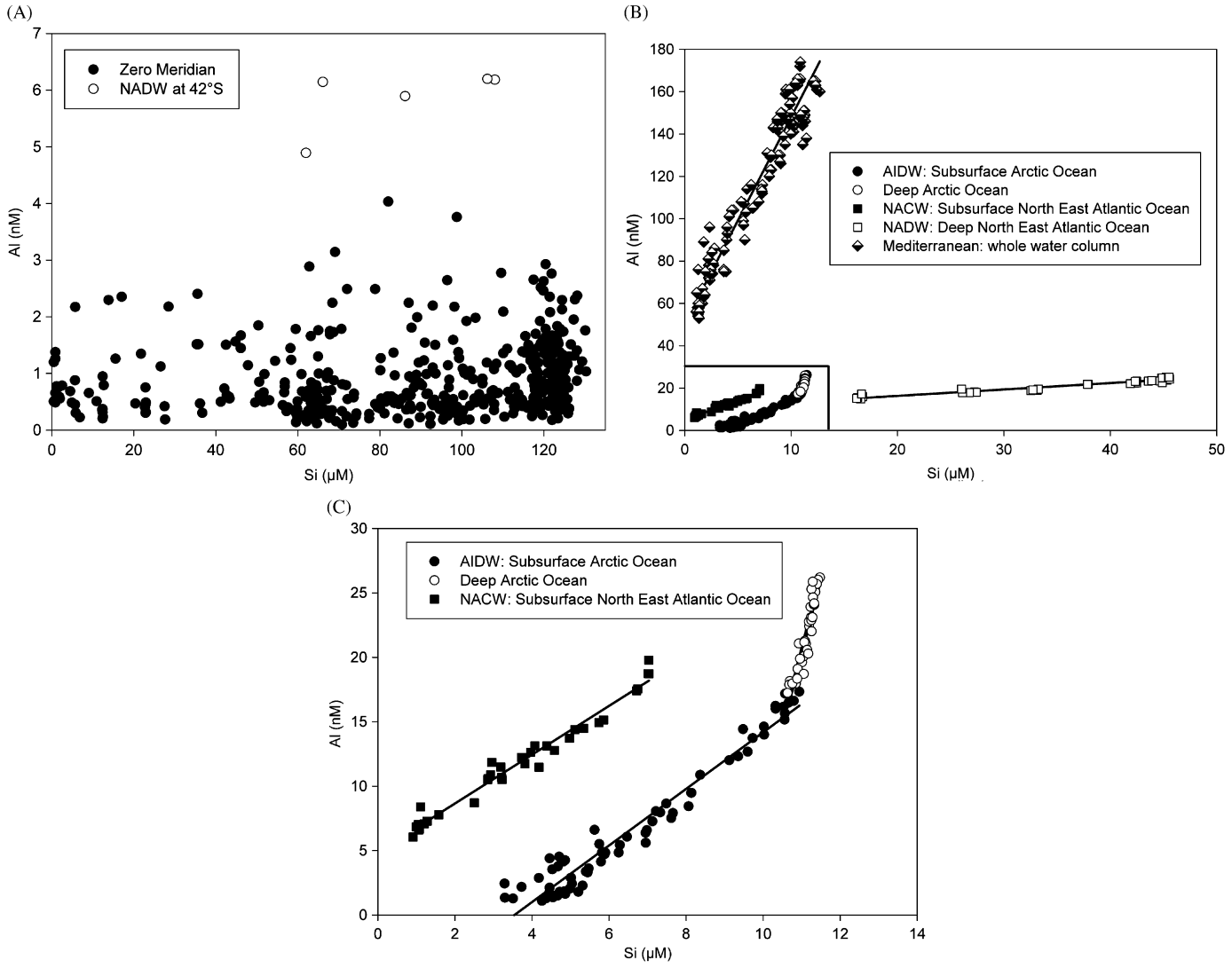

Fig. 8. (A) Concentrations of Al (nM) versus concentrations of silicate (μM) for the whole water column from all 22 TM stations in the South East Atlantic Ocean and along the zero meridian. No relation was observed between Al and Si, with the exception of a trend in the NADW (< 2000 m depth) at 42°20′S, 9°E, in the Sub-Antarctic Zone. The trend can be described by [Al][nM] = 0.02[Si][μM] + 4.6 with $R^2 = 0.3$, $n = 5$, but is not a significant correlation ($P = 0.3$). (B) Concentrations of Al (nM) versus concentrations of silicate (μM) in the Arctic Ocean, North East Atlantic Ocean and the Mediterranean Sea. A relationship between Al and Si was observed in the Atlantic and Intermediate Water (AIDW) in the subsurface Arctic Ocean; in the deep Arctic Ocean; in the North Atlantic Central Water (NACW); in the subsurface North East Atlantic Ocean; in the North Atlantic Deep Water (NADW; in the deep North East Atlantic Ocean; and over the whole water column of the Mediterranean Sea. The Arctic correlations are described by [Al][nM] = 2.2[Si][μM] − 8.5 with $R^2 = 0.95$, $n = 68$ and $P < 0.0001$ for the AIDW and by [Al][nM] = 10.3[Si][μM] − 92 with $R^2 = 0.85$, $n = 39$ and $P < 0.0001$ for the deep Arctic Ocean (for further details see Middag et al. (2009)). The North East Atlantic Ocean correlations are described by [Al][nM] = 1.9[Si][μM] + 4.9 with $R^2 = 0.97$, $n = 36$ and $P < 0.0001$ for the NACW and by [Al][nM] = 0.3 [Si][μM] + 11.3 with $R^2 = 0.92$ $n = 20$ and $P < 0.0001$ for the NADW (results from 39°44′N, 14°10′W; (Middag et al., 2010)). The Mediterranean correlation is described by [Al][nM] = 9.8[Si][μM] + 50 with $R^2 = 0.94$, $n = 141$ and $P < 0.0001$ (data from Hydes et al., 1988). Inset is shown at expanded scale in Fig. 8C. (C) Concentrations of Al (nM) versus concentrations of silicate (μM) in the AIDW, deep Arctic Ocean and NACW at expanded scale.

2×10^{-3} in the AIDW (Middag et al., 2009). As a result upon export and dissolution, the dissolved Al increases only modestly with increase in depth, as observed in the Weddell Basin from 0.2 nM Al in the subsurface minimum at about 100–150 m depth to 0.77–0.98 nM at 4000 m depth in the WSDW.

Besides inputs and export of Al and Si, the Al–Si cycling is also affected by deep ocean circulation. The residence time of Si (in the order of 16,000 years; Sarmiento and Gruber, 2006, p. 310) exceeds the approximate 2000-year ventilation time of the oceans, while the residence time of Al is considerably shorter (50–200 years). The particle-reactive nature of Al causes a rapid removal of Al from deep waters, while Si is 'inert' and therefore left behind in deep waters. Thus the two biogeochemical cycles become decoupled during deep ocean circulation. This is confirmed when following the circulation of NADW. The deep Arctic Ocean is an important source of NADW (Rudels et al., 2000) and has a relatively high Al/Si ratio of about 10×10^{-3} (see text above). Following the NADW on its way south, in the North East Atlantic Ocean the ratio derived from the Al–Si relation already has decreased over one order of magnitude from around 10×10^{-3} to 0.3×10^{-3} (Fig. 8B). In the NADW in the South East Atlantic Ocean at our most northerly station (42°20′S, 9°E), there is no significant correlation between Al and Si ($P = 0.3$; Fig. 8A). Nevertheless, the slope of this relation of 0.02×10^{-3} would be another order of magnitude lower than the slope of the relation observed in the North East Atlantic Ocean. The transit time of the NADW from its origin in the Nordic oceans to our station at 42°20′S, 9°E, is in the order of 200 years (Broecker et al., 1998). This transit time exceeds or equals the residence time of Al, implying that upon arrival of NADW at 42°S virtually all Al of

Nordic origin has disappeared, implying that the deep concentrations of Al at 42°S are the result of relatively recent 'underway' inputs of mixing and surface export during the journey of the NADW. This explains the relatively low concentration of Al (~6 nM) observed in the NADW at 42°S compared to a concentration of about 18 nM in the deep North Atlantic Ocean (Hall and Measures, 1998). In contrast the concentrations of Si at 42°S are the result of (virtually all) the 'original' Si concentration in the NADW in the North Atlantic Ocean plus (virtually all of) the 'underway' inputs from the 200-year journey of the NADW. This can be seen in the increase in the concentration of Si from below 20 μM in NADW in the North Atlantic Ocean (Hall and Measures, 1998) to about 80 μM at the station at 42°S.

Summarising, in some other deep oceans a relation between Al and Si is observed but not here in the deep Southern Ocean. We suggest the Al–Si relation is apparent in deeper waters when the Al and Si supplied to the surface layer are proportional with the Al:Si ratio of the exported diatom opal (biogenic silica). In the Southern Ocean hardly any Al is supplied but Si is available in large excess. This causes a much lower Al:Si ratio for local biogenic silica. When this is exported and next dissolves in the deep ocean, the ensuing Al/Si signal is too small to detect against the high Si and low Al background concentrations. Moreover, the Al–Si relation gets further uncoupled in the deep ocean due to scavenging removal of dissolved Al while dissolved Si is left behind, thus yielding the much shorter deep ocean residence time of Al (50–200 years) compared to Si (~16,000 years).

5. Conclusions

The complete section of the Antarctic Circumpolar Current and Weddell Gyre is the first comprehensive assessment of the distribution of Al in the Southern Ocean and shows that the actual concentrations are lower than most previous reports. Further improvement of global simulation models that use surface concentrations of Al to constrain dust deposition to the oceans is now feasible. The distribution of Al in the surface of the Southern Ocean suggests that the upper surface is slightly elevated by atmospheric input, which is due to a combination of direct atmospheric (wet and dry) input and indirect atmospheric input via melting sea ice. Melting from continental ice also influences the distribution of Al in the surface ocean, but only close to the edge of the continental ice-sheet or close to melting icebergs. The distribution of Al in the intermediate and deep Southern Ocean is mainly the result of mixing of water masses with different origins, deep water formation and additional input from sedimentary sources at sea floor elevations. No apparent relation was observed between Al and Si in the Southern Ocean. We have argued that the relation between Al and Si, as observed in the water column of some other ocean regions, is apparent in the deeper water layers when the Al and Si supplied to the surface layer are proportional with the Al:Si uptake ratio of diatoms. Upon export of the diatom particles into underlying subsurface waters the siliceous diatom frustules dissolve with the same ratio, thus imprinting the Al:Si ratio of biogenic silica in the dissolved Al/Si ratio. In the Southern Ocean, the biogenic silica has a much lower Al:Si ratio due to the limited input of Al and when this biogenic silica dissolves in the deep ocean the resulting Al/Si signal is too small to detect against the high Si and low Al background concentrations. Moreover, the Al–Si relation gets further distorted in the deep ocean due to the different chemistries and resulting residence times, uncoupling the Al–Si relation. Here it is envisioned that the particle-reactive nature of Al versus 'inert' silicate causes a rapid removal of Al from deep waters while dissolved silicate is left behind in deep waters.

Acknowledgments

The authors are most grateful to the master S. Schwarze and crew of R.V. Polarstern for their splendid support during the expedition. Special thanks to Sven Ober for the operation of the all-titanium CTD sampling system for trace metals. Sven Ober was assisted by Willem Polman who, together with the pilot, tragically lost his live during this expedition in a helicopter accident. His help and support were invaluable, as were his personality and presence. Willem Polman will therefore live on in our memories. After this tragic loss Michal Stimac stepped up to help with the operation of the TM sampling system. For this we are most grateful, as without his efforts we would not have been able to continue our work in the memory of the colleagues we lost. Much gratitude to Loes Gerringa for her constructive comments, my colleagues Maarten Klunder and Charles-Edouard Thuróczy for their help with sampling and general support. Finally, I would like to express a lot of gratitude to all participants of cruise ANT XXIV/3, for their help and support during this memorable expedition. Constructive comments of three reviewers and the associate editor are appreciated and have led to significant improvements of the manuscript. This work was funded by NWO Geotraces subproject: 851.40.101.

Appendix A. Supporting information

Supplementary data associated with this article can be found in the online version at doi:10.1016/j.dsr2.2011.03.001.

References

Abouchami, W., Galer, S.J.G., De Baar, H.J.W., Alderkamp, A.C., Middag, R., Laan, P., Feldmann, H., Andreae, M.O.. Modulation of the Southern Ocean cadmium isotope signature by ocean circulation and primary productivity. Earth and Planetary Science Letters, in press, doi:10.1016/j.epsl.2011.02.044.

Baars, O., Croot, P.L., 2011. The speciation of dissolved zinc in the Atlantic sector of the Southern Ocean. Deep-Sea Research II 58, 2720–2732.

Barré, N., Provost, C., Sennechael, N., Lee, J.H., 2008. Circulation in the Ona Basin, southern Drake Passage. Journal of Geophysical Research 113 (C4), C04033.

Broecker, W.S., Peacock, S.L., Walker, S., Weiss, R., Fahrbach, E., Schroeder, M., Mikolajewicz, U., Heinze, C., Key, R., Peng, T.H., Rubin, S., 1998. How much deep water is formed in the Southern Ocean? Journal of Geophysical Research 103 (C8), 15833–15843.

Brown, M.T., Bruland, K.W., 2008. An improved flow-injection analysis method for the determination of dissolved aluminum in seawater. Limnology and Oceanography Methods 6, 87–95.

Bruland, K.W., Orians, K.J.., Cowen, J.P., 1994. Reactive trace metals in the stratified North Pacific. Geochimica et Cosmochimica Acta 58 (15), 3171–3182.

Chou, L., Wollast, R., 1997. Biogeochemical behavior and mass balance of dissolved aluminium in the western Mediterranean Sea. Deep-Sea Research II 44 (3–4), 741–768.

Collier, R., Edmond, J., 1984. The trace element geochemistry of marine biogenic particulate matter. Progress in Oceanography 13 (2), 113–199.

Croot, P.L., Baars, O., Streu, P., 2011. The distribution of dissolved zinc in the Atlantic sector of the Southern Ocean. Deep-Sea Research II 58, 2707–2719.

De Baar, H.J.W., Timmermans, K.R., Laan, P., de Porto, H.H., Ober, S., Blom, J.J., Bakker, M.C., Schilling, J., Sarthou, G., Smit, M.G., Klunder, M., 2008. Titan: a new facility for ultraclean sampling of trace elements and isotopes in the deep oceans in the international Geotraces program. Marine Chemistry 111 (1–2), 4–21.

Duce, R.A., Tindale, N.W., 1991. Atmospheric transport of iron and its deposition in the ocean. Limnology and Oceanography 36 (8), 1715–1726.

Gehlen, M., Beck, L., Calas, G., Flank, A.M., Van Bennekom, A.J., Van Beusekom, J.E.E., 2002. Unraveling the atomic structure of biogenic silica: evidence of the structural association of Al and Si in diatom frustules. Geochimica et Cosmochimica Acta 66 (9), 1604–1609.

Gehlen, M., Heinze, C., Maier-Reimer, E., Measures, C.I., 2003. Coupled Al–Si geochemistry in an ocean general circulation model: a tool for the validation of oceanic dust deposition fields? Global Biogeochemical Cycles 17 (1), 1028.

GEOTRACES Planning Group, 2006. GEOTRACES Science Plan. Scientific Committee on Oceanic Research, Baltimore, Maryland.

Grasshoff, K., Erhardt, M., Kremling, K., 1983. Methods in Seawater Analyses. Verlag Chemie, Weinheim, Germany 419pp.

Hall, I.R., Measures, C.I., 1998. The distribution of Al in the IOC stations of the North Atlantic and Norwegian Sea between 52° and 65° North. Marine Chemistry 61 (1–2), 69–85.
Han, Q., Moore, J.K., Zender, C., Measures, C., Hydes, D., 2008. Constraining oceanic dust deposition using surface ocean dissolved Al. Global Biogeochemical Cycles 22 (2), GB2003.
Hydes, D.J., 1977. Dissolved aluminium in sea water. Nature 268 (5616), 136–137.
Hydes, D.J., 1979. Aluminium in seawater: control by inorganic processes. Science 205 (4412), 1260–1262.
Hydes, D.J., de Lange, G.J., de Baar, H.J.W., 1988. Dissolved aluminum in the Mediterranean. Geochimica et Cosmochimica Acta 52 (8), 2107–2114.
Johnson, K.S., Boyle, E., Bruland, K., Measures, C., Moffett, J., Aquilarislas, A., Barbeau, K., Cai, Y., Chase, Z., Cullen, J., Doi, T., Elrod, V., Fitzwater, S., Gordon, M., King, A., Laan, P., Laglera-Baquer, L., Landing, W., Lohan, M., Mendez, J., Milne, A., Obata, H., Ossiander, L., Plant, J., Sarthou, G., Sedwick, P., Smith, G.J., Sohst, B., Tanner, S., Van Den Berg, S., Wu, J, 2007. Developing standards for dissolved iron in seawater. EOS, Transactions American Geophysical Union 88 (11), 131–132.
Klatt, O., Fahrbach, E., Hoppema, M., Rohardt, G., 2005. The transport of the Weddell Gyre across the Prime Meridian. Deep-Sea Research II 52 (3–4), 513–528.
Klunder, M., Laan, P., Middag, R., De Baar, H.J.W., Van Ooijen, J.C., 2011. Dissolved Fe in the Southern Ocean (Atlantic Sector). Deep-Sea Research II 58, 2678–2694.
Kramer, J., Laan, P., Sarthou, G., Timmermans, K.R., de Baar, H.J.W., 2004. Distribution of dissolved aluminium in the high atmospheric input region of the subtropical waters of the North Atlantic Ocean. Marine Chemistry 88 (3-4), 85–101.
Ligi, M., Bonatti, E., Bortoluzzi, G., Carrara, G., Fabretti, P., Gilod, D., Peyve, A.A., Skolotnev, S., Turko, N., 1999. Bouvet Triple Junction in the South Atlantic: geology and evolution. Journal of Geophysical Research 104 (B12), 29,365–29,385.
Mackenzie, F.T., Stoffyn, M., Wollast, R., 1978. Aluminum in seawater: control by biological activity. Science 199 (4329), 680–682.
Mackin, J.E., Aller, R.C., 1984. Processes affecting the behavior of dissolved aluminum in estuarine waters. Marine Chemistry 14 (3), 213–232.
Maring, H.B., Duce, R.A., 1987. The impact of atmospheric aerosols on trace metal chemistry in open ocean surface seawater, 1, aluminum. Earth and Planetary Science Letters 84 (4), 381–392.
Measures, C.I., Edmond, J.M., 1990. Aluminum in the South-Atlantic—steady-state distribution of a short residence time element. Journal of Geophysical Research, Oceans 95 (C4), 5331–5340.
Measures, C.I., Edmond, J.M., 1992. The distribution of aluminium in the Greenland Sea and its relationship to ventilation processes. Journal of Geophysical Research, Oceans 97 (C11), 17787–17800.
Measures, C.I, 1995. The distribution of Al in the IOC stations of the Eastern Atlantic between 30-degrees-S and 34-degrees-N. Marine Chemistry 49 (4), 267–281.
Measures, C.I, 1999. The role of entrained sediments in sea ice in the distribution of aluminium and iron in the surface waters of the Arctic Ocean. Marine Chemistry 68 (1–2), 59–70.
Measures, C.I., Brown, M.T., Vink, S., 2005. Dust deposition to the surface waters of the western and central North Pacific inferred from surface water dissolved aluminum concentrations. Geochemistry Geophysics Geosystems 6 (9), Q09M03.
Middag, R., 2010. Dissolved Aluminium and Manganese in the Polar Oceans. Ph.D. Thesis. University of Groningen, Groningen, The Netherlands.
Middag, R., De Baar, H.J.W., Laan, P., Bakker, K., 2009. Dissolved aluminium and the silicon cycle in the Arctic Ocean. Marine Chemistry 115 (3–4), 176–195.
Middag, R., De Baar, H.J.W., Laan, P., Cai, P.H., Van Ooijen, J.C., 2011. Dissolved manganese in the Atlantic Sector of the Southern Ocean. Deep-Sea Research II 58, 2661–2677.
Moore, R.M., Millward, G.E., 1984. Dissolved-particulate interactions of aluminium in ocean water. Geochimica et Cosmochimica Acta 48 (2), 235–241.
Moran, S.B., Moore, R.M., 1991. The potential source of dissolved aluminium from resuspended sediments to the North Atlantic Deep Water. Geochimica et Cosmochimica Acta 55 (10), 2745–2751.
Moran, S.B., Moore, R.M., Westerlund, S., 1992. Dissolved aluminum in the Weddell Sea. Deep-Sea Research 39 (3–4), 537–547.
Orians, K.J., Bruland, K.W., 1985. Dissolved aluminum in the Central North Pacific. Nature 316 (6027), 427–429.
Orians, K.J., Bruland, K.W., 1986. The biogeochemistry of aluminum in the Pacific-Ocean. Earth and Planetary Science Letters 78 (4), 397–410.
Resing, J., Measures, C.I., 1994. Fluorimetric determination of Al in seawater by FIA with in-line preconcentration. Analytical Chemistry 66 (22), 4105–4111.
Rudels, B., Muench, R.D., Gunn, J., Schauer, U., Friedrich, H.J., 2000. Evolution of the Arctic Ocean boundary current north of the Siberian Shelves. Journal of Marine Systems 25 (1), 77–99.
Sarmiento, J.L., Gruber, N., 2006. Ocean Biogeochemical Dynamics. Princeton University Press, Princeton, New Jersey, p. 310.
Stoffyn, M., 1979. Biological control of aluminium in seawater: experimental evidence. Science 203 (4381), 651–653.
Thuróczy, C-E., Gerringa, L.J.A., Klunder, M.B., Laan, P., De Baar, H.J.W., 2011. Observation of consistent trends in the organic complexation of dissolved iron in the Atlantic sector of the Southern Ocean. Deep-Sea Research II 58, 2695–2706.
Tria, J., Butler, E.C.V., Haddad, P.R., Bowie, A.R., 2007. Determination of aluminium in natural water samples. Analytica Chimica Acta 588 (2), 153–165.
Van Bennekom, A.J., Jansen, F., Van Der Gaast, S., Van Iperen, J., Pieters, J., 1989. Aluminum-rich opal: an intermediate in the preservation of biogenic silica in the Zaire (Congo) deep-sea fan. Deep-Sea Research Part A 36 (2), 173–190.
Van Bennekom, A.J., Buma, A.G.J., Nolting, R.F., 1991. Dissolved aluminium in the Weddell–Scotia Confluence and effect of Al on the dissolution kinetics of biogenic silica. Marine Chemistry 35 (1–4), 423–434.
Van Beusekom, J.E.E., Weber, A., 1992. Decreasing diatom abundance in the North Sea: the possible significance of aluminium. In: Colombo, G. (Ed.), Marine Eutrophication and Population Dynamics. Olsen and Olsen, Fredensborg, Denmark, pp. 121–127.
Van Beusekom, J.E.E., van Bennekom, A.J., Tréguer, P., Morvan, J., 1997. Aluminium and silicic acid in water and sediments of the Enderby and Crozet Basins. Deep-Sea Research II 44 (5), 987–1003.
Whitworth, T., Nowlin, W.D., 1987. Water masses and currents of the Southern-Ocean at the Greenwich Meridian. Journal of Geophysical Research 92 (C6), 6462–6476.